

MUTUAL VALIDATION BETWEEN EFD/CFD FOR SUPERSONIC FLOW AROUND NEXST-1

Ryoji Takaki , Norio Suzuki , Kenji Yoshida
Japan Aerospace Exploration Agency
Institute of Space Technology and Aeronautics
7-44-1 Jindaiji-Higashi, Chofu, Tokyo, 182-8522 JAPAN

Keywords: *CFD, validation, supersonic*

Abstract

This paper presents a detailed comparison of EFD/CFD results for the supersonic flow around NEXST-1. The CFD results show fairly good agreement with each other as well as the experimental data except for following discrepancies: C_D , $C_{L\alpha}$, $C_{M\alpha}$ and the pressure distributions at the leading edge on the upper surface as well as at the outer wing. Detailed studies on the above discrepancies were conducted as follows: sensitivity analysis for parameters of the experiments, repeatability check of the experimental data, geometry measurement of the wind tunnel model, aeroelasticity analysis of the wind tunnel model, and effects of transition. The results show that the discrepancies of $C_{L\alpha}$ and $C_{M\alpha}$ are caused by the aeroelastic deformation of the wind tunnel mode. Also the discrepancy of the pressure distributions are caused by the difference of the model geometry and the transition specification.

1 Introduction

Japan Aerospace Exploration Agency (JAXA) has conducted NEXST (National EXperimental Supersonic Transport) project[1]. This project aims to establish an optimal design system for a next generation supersonic transport based on Computational Fluid Dynamics (CFD). Highly reliable CFD codes are indispensable for using CFD as an optimal design tool. It has been suggested that aerodynamic drag prediction er-

ror should be less than 1 count. Therefore, more systematic and precise validation and verification are necessary for enhancement of CFD reliability. For this purpose, the 3rd SST-CFD-Workshop[2] was held in Dec. 2001, where verification and validation of CFD results for NEXST-1 8.5% scale model were conducted. It was pointed out that further investigation is necessary for several differences between the CFD results and the experimental data. This paper summarizes the discussion at the workshop and reports mutual validation results on discrepancy between the CFD results and the experimental data, which were conducted after the workshop.

2 SST-CFD-Workshop

The subjects of the workshop for supersonic flow analysis around NEXST-1 consists of two parts. One is analysis of a wind tunnel testing condition and another is that of a real flight condition of the experimental vehicle. Attack angle sweep are required for both conditions. Dimensions of the experimental vehicle and calculation conditions are listed in Table 1 and Table 2, respectively. The wind tunnel model is a 8.5% scaled model of the real experimental vehicle but the geometry of the model is different at the boat tail because of the installation to the sting of the wind tunnel. The boat tail of the model is cut off at the station 0.79 m from the nose, right behind the vertical wing. Figure 1 shows the 8.5% scaled model, installed to a wind tunnel at ISTA/JAXA.

The experimental data used in this validation are as follows; longitudinal aerodynamic characteristics: C_L , C_D and C_M , and pressure distributions at each span location: 30%, 50%, 70% and 90%.



Fig. 1 8.5% scaled model of NEXST-1

Table 1 Dimensions of NEXST-1

Dimensions	Values
Length [m]	11.5
Wing span [m]	4.718
Reference area [m^2]	10.117
Longitudinal reference length [m]	2.754
Momentum center [m]	(5.254, 0, 0)

Table 2 Numerical conditions

Parameters	Values
Unit Reynolds number	27.5×10^6
Mach number	2.0
Attack angle [degree]	-2, -1, 0, 1, 2, 3, 4, 5, 6
Misc	Forced transition at the leading edge

Table 3 is the list of the numerical methods used by each applicant. There are several kinds of turbulence models and numerical grids: structured grid and unstructured grid.

Comparison between the CFD results and the experimental data was conducted. The details of both data were written in the previous paper[3].

2.1 Comparison of Aerodynamic characteristics

First, we discuss about aerodynamic characteristics. Figure 2(a), 2(b) and 2(c) show diagram of $\alpha - C_L$, $\alpha - C_M$ and $C_D - C_L$, respectively. Table 4 shows coefficients of curve fitted approximation for each aerodynamic coefficient: C_L , C_M and C_D . The curve fitting is conducted between the attack angle of -2 and 2 .

First we compare the CFD results with each other. As for C_L , the CFD results show good agreement. As for C_M , the CFD results show good agreement except for a small difference of $C_{M\alpha}$, which causes none negligible difference of C_M at high angle attack cases. As for C_D , a big discrepancy can be seen. For example, the discrepancy of C_{Dmin} is up to 20 counts.

Next, the CFD results are compared with the experimental data. As for C_L , the CFD results show good agreement except for a slight difference of $C_{L\alpha}$, where the CFD results is a little bit higher than the experimental data. Regarding C_M , which is similar to C_L , they show good agreement as a whole except for $C_{M\alpha}$ where the CFD results is a little bit smaller than the experimental data. As for C_D , it is difficult to compare the CFD results with the experimental data because the CFD results show big deviations in themselves. The discrepancy between the CFD results and the experimental data is about ± 10 counts.

Then we compared coefficients for curve fitted approximation of each aerodynamic coefficient, excepting the maximum and the minimum value of the CFD results. As for C_L , differences are as follows; from 4% to 7% for $C_{L\alpha}$ and 2% to 4% (less than 0.04 degree) for α_0 . As for C_M , differences are as follow; from 6% to 9% for $C_{M\alpha}$ and 13% to 26% for C_{M0} , which are bigger than C_L case. Regarding C_D , differences are as follows; from 2% to 7% for K , 17% to 51% for C_{L0} and 2% to 8% (2 to 9 in counts) for C_{Dmin} . The difference of C_{L0} is bigger than that of K and C_{Dmin} .

Table 3 Workshop applicants

ID	Applicant(Organization)	Governing equation	Grid(points)	Turbulence model
SST01	K. Miyaji(Yokokoku Univ.)	NS	USG:tetra+prism(0.9M)	k- ω
SST02	M. Yoshimoto(MHI)	NS(TL)	SBSG(1.5M)	B-L
SST03	Y. Ito(Tohoku Univ.)	NS	USG:tetra+prism(1M)	G-R
SST04	M. Kondo(Tohoku Univ.)	NS(TL)	MBSG(2.3M)	B-L
SST05	UPACS-BL(ISTA/JAXA)	NS	MBSG(3.4M)	B-L
SST06	UPACS-SA(ISTA/JAXA)	NS	MBSG(2.3M)	S-A
SST07	A. Ochi(KHI)	NS	USG:hexa(0.9M)	B-B
SST08	P. Lahur(Nagoya Univ.)	Euler	Cartesian(0.5M)	NO
-	U. Herrmann(DLR)	NS	unknown	unknown
-	M. Kubosawa(FHI)	Euler+BLC	Cartesian	L-E

B-L : Baldwin-Lomax, S-A : Spalart-Allmaras, G-R : Goldberg-Ramakrishnan,

L-E : Green’s Lag-Entrainment, B-B : Baldwin-Barth

TL : Thin layer, BLC : Boundary layer correction

MBSG : Multi-Block structured grid, USG : Unstructured grid, SBSG : Single-Block structured grid

Table 4 Comparison of the aerodynamic characteristics

	C_L		C_M		C_D		
	$C_L = C_{L\alpha}(\alpha - \alpha_0)$		$C_M = C_{M\alpha}\alpha + C_{M0}$		$C_D = K(C_L - C_{L0})^2 + C_{Dmin}$		
	$C_{L\alpha}$	α_0	$C_{M\alpha}$	C_{M0}	K	C_{L0}	C_{Dmin}
SST01	0.0370	-0.946	-0.0126	-0.00729	0.459	0.00774	0.0111
SST02	0.0371	-0.933	-0.0128	-0.00774	0.417	0.00509	0.0108
SST03	0.0377	-0.924	-0.0129	-0.00831	0.457	0.00919	0.0122
SST04	0.0366	-0.913	-0.0123	-0.00580	0.425	0.00528	0.0128
SST08	0.0380	-0.826	-0.0127	-0.00784	-	-	-
SST05	0.0375	-0.932	-0.0129	-0.00771	0.415	0.00552	0.0106
SST06	0.0376	-0.929	-0.0131	-0.00794	0.400	0.00390	0.0111
Experiment(1999)	0.0354	-0.951	-0.0119	-0.00629	0.428	0.00789	0.0113

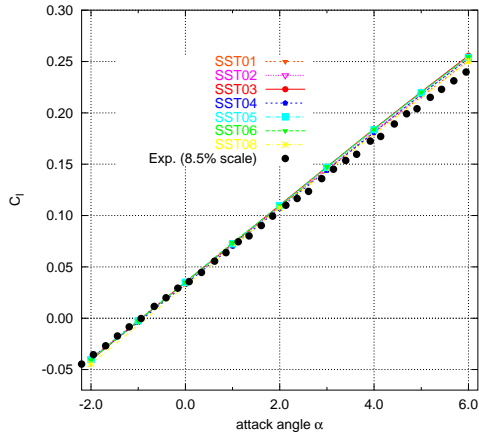
2.2 Comparison of pressure distributions on the wing

Here, a comparison of pressure distributions on the wing is described. Figure 3 shows an example of the comparison. The CFD results are compared with each other, showing excellent agreement except for some small differences. Then the CFD results are also compared to the experimental data, showing fairly good agreement as a whole. However, there are two remarkable discrepancies. One is how to capture a suction peak at the upper surface of the leading edge, which is remarkable at the 50% span location close to the

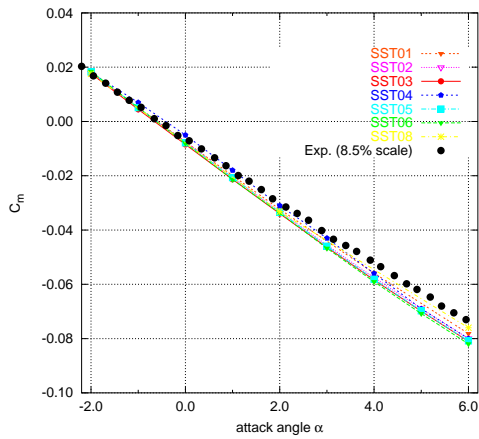
leading edge kink. Another big discrepancy is at the outer wing region.

2.3 Subjects for further investigations

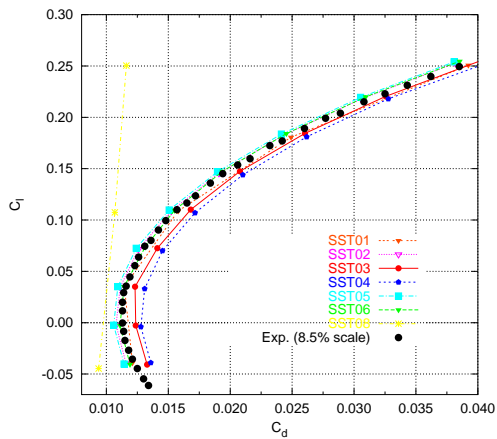
Here we summarize the results of comparisons and conclude as follows. Regarding the aerodynamic characteristics, except for C_D , and pressure distributions, the CFD results show fairly good agreement with each other as well as the experimental data. As for $C_{L\alpha}$ and $C_{M\alpha}$, There is the small difference between the CFD results and the experimental data. C_D is also a issue to be discussed further. As for pressure distributions, fol-



(a) Lift coefficient (C_L)

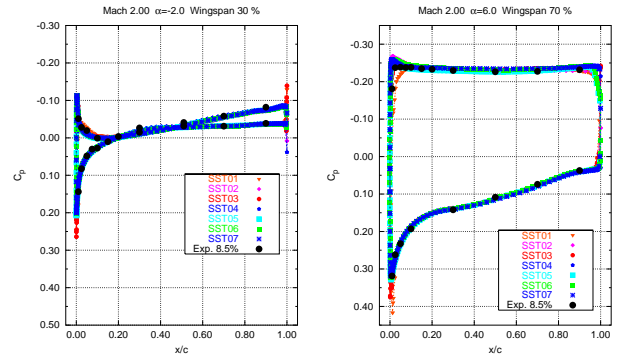


(b) Pitching moment coefficient (C_M)



(c) Drag polars

Fig. 2 Comparison of the aerodynamic characteristics



(a) $\alpha = -2$ and $y/b = 30\%$ (b) $\alpha = 6$ and $y/b = 70\%$

Fig. 3 Examples of the pressure distributions

lowing two aspects should be discussed further. One is at the leading edge on the upper surface at 50% span location (Fig.4(a)) and another is at the outer wing region (Fig.4(b)). The discrepancy at 50% span location is remarkable for the design condition as attack angle is 2.0. Therefore detailed investigation was conducted for following discrepancies, $C_{L\alpha}$, $C_{M\alpha}$ and pressure distributions at the leading edge of the 50% span location and at the 90% span location in the case of $\alpha = 2$.

3 Detailed study on the discrepancy

Detailed study on the discrepancies was conducted between the CFD results and the experimental data. UPACS solver[4], which is a standard CFD program at ISTA/JAXA, was used. Navier-Stokes equations are discretized in the manner of cell-centered finite volume method in UPACS solver. UPACS solver is a typical CFD program for compressible flow simulations, which consist of Multi-block structured grid method, Roe's Riemann solver with MUSCL approach, and Baldwin-Lomax (BL) model and Spalart-Allmaras (SA) model as a turbulence model.

3.1 Dependency on grids and numerical methods

First of all, dependency checks on computational grids and numerical schemes were studied. The grid dependency check[5] shows sufficient

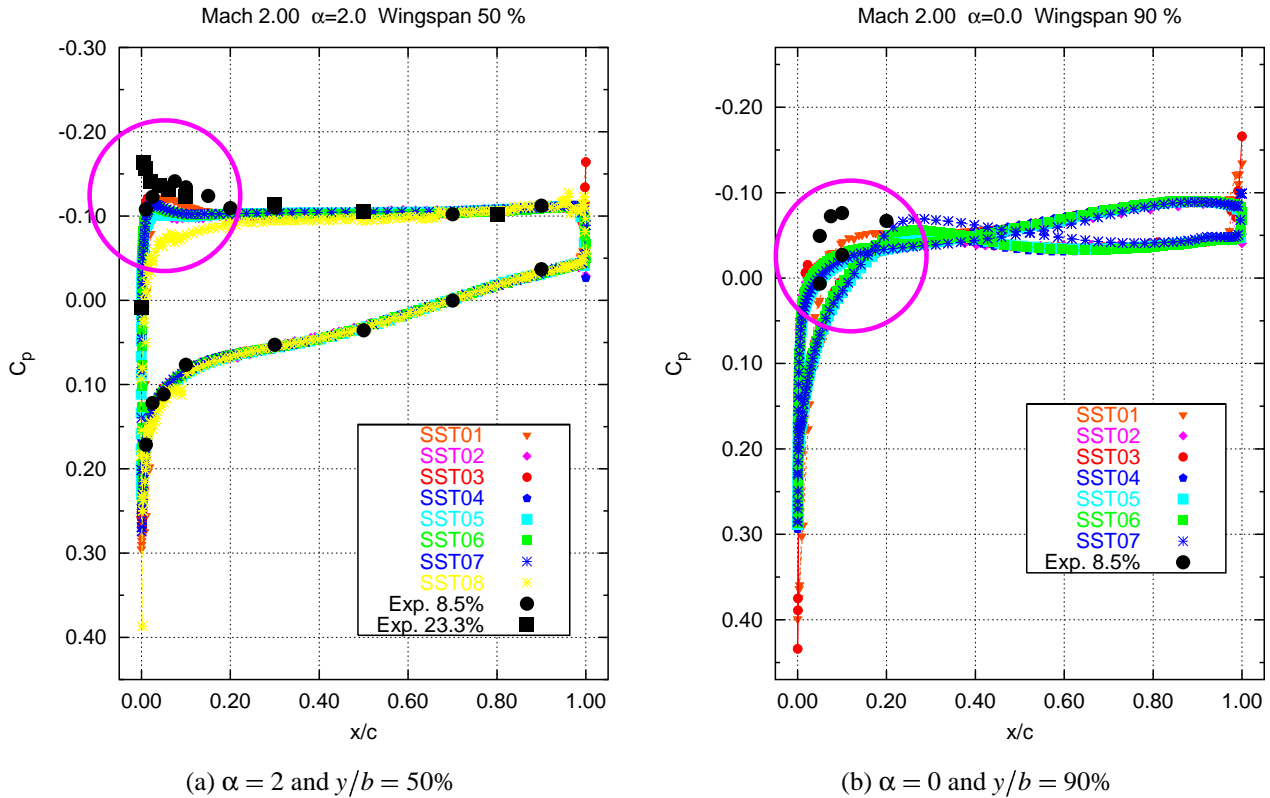


Fig. 4 Comparison of the pressure distributions

grid convergence for the current number of grid points. The number of grid points are 2.3 million for BL model analysis and 3.4 million for SA model analysis. The dependency check[3] for limiter functions for MUSCL approach shows no remarkable difference among limiters except for *superbee*. Here, *minmod*, *superbee*, *van Albada* and *van Leer* for 2nd order accuracy and *minmod* for 3rd order accuracy were used as limiter functions. *Superbee* can capture suction peak sharply because of relative low artificial viscosity. However, it does not affect the pressure distributions so much.

3.2 Sensitivity analysis for parameters of the experiment

Sensitivity analysis was conducted for parameters of wind tunnel operations using CFD because one of the uncertainty of the experimental data comes from setting error of them. Free stream Mach number and angle of attack were considered. As for Mach number, 1.96 and 2.04 are

studied for the right condition of 2.0. As for attack angle, 1.8, 2.2 and 2.4 are studied for the right condition of 2.0. Figure 5 and 6 show the results of sensitivity analysis for Mach number and attack angle, respectively. The pressure distributions at the leading edge on the upper surface are sensitive not to free stream Mach number but to attack angle. It is true that pressure distributions at that region is sensitive to attack angle but used deviation is too large and it exceeds general setting error of attack angle greatly. Therefore the difference of the pressure distributions is not caused only by the setting error of attack angle.

Still we cannot decrease the difference of the aerodynamic characteristics and the pressure distributions between the CFD results and the experimental data. Therefore we conducted following studies: repeatability of the experimental data, model geometry, turbulent transition and elastic deformation, presented in Fig. 8 and 9. Figure 8 shows the aerodynamic characteristics and Fig. 9 shows the pressure distributions which are fo-

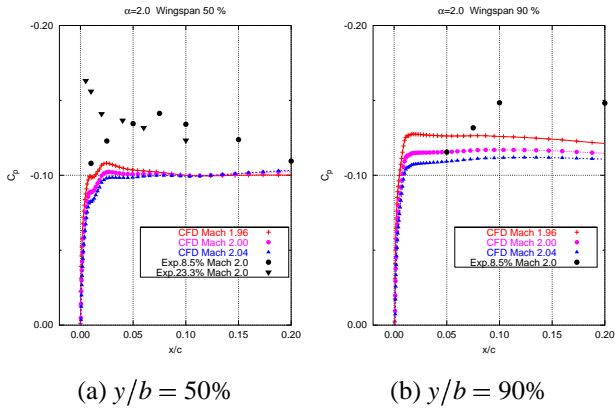


Fig. 5 Comparison of the pressure distributions at the leading edge (dependency on free stream Mach number)

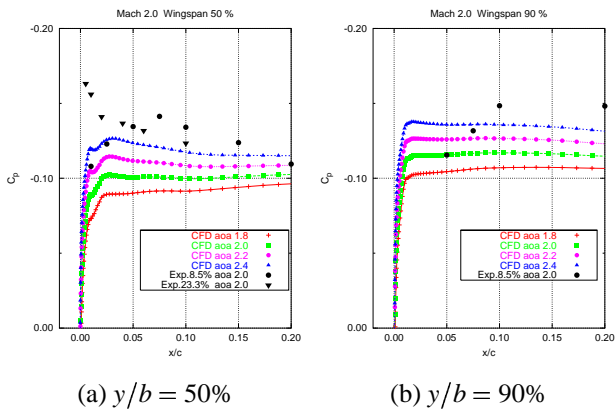


Fig. 6 Comparison of the pressure distributions at the leading edge (dependency on angle of attack)

cused on.

3.3 Repeatability of the experimental data

Two kinds of the experimental data in Fig. 9(a) show different tendency with each other. It is worthy of note that difference of the experimental data is not pressure level but distribution tendency. Discrepancy between two experimental data is larger than that among the CFD results. Some problems seems to exist in these experiments, where the wind tunnels and the size of the wind tunnel models were different from each other. The experiment using the 8.5% scaled model was conducted JAXA’s supersonic wind tunnel in 1999 and the experiment using the

23.3% scaled model was conducted at ONERA. Thus the differences between the 8.5% and the 23.3% scaled models are as follows; the model manufacturers, the purpose of the model (consequently accuracy requirements) and the wind tunnels.

Regarding the 8.5% scaled model, another wind tunnel test was conducted at newly improved supersonic wind tunnel at JAXA in 2002 to check repeatability of the experimental data[6]. Regarding comparison between two experiments at JAXA, the results show about 10 counts difference for C_D shown in Fig.8. The repeatability of the C_D at the newly improved wind tunnel is about 2 counts. Other aerodynamic characteristics C_L and C_M show good agreement. Difference of C_D between two experiments is almost the same as that between the CFD results and the experimental data. The difference between two experimental data of 1999 and 2002 is relatively bigger than usual because of the improvement of the wind tunnel, persons in charge, long interval of the experiments and disk roughness used as the method of fixing the transition point, which is relatively lower repeatability.

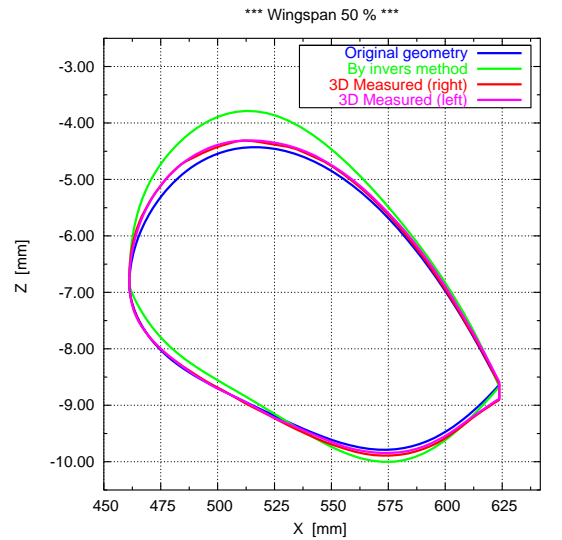
3.4 Geometry measurement of the wind tunnel model

We applied an inverse method to estimate the geometry of the wind tunnel model that produces the experimental pressure distributions[7]. As for comparison between the original geometry and the estimated geometry by the inverse method, the results show that extremely small difference, which is same level of manufacturing accuracy, changes the pressure distributions around the leading edge at the 50% span location greatly. Therefore the geometry measurement was carried out by a three-dimensional non-contact measuring device employing laser beam and auto-focus system. The measuring accuracy is 0.1 micron. The leading edge, which is most important and the trailing edge could not be measured sufficiently. Because the measuring device cannot capture reflection of laser beam due to the large curvature around the leading edge. For ex-

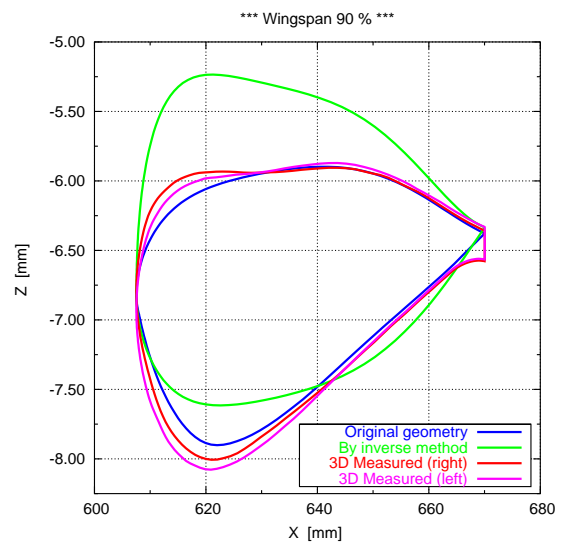
ample, the region from the leading edge to 3% chord length could not be measured at the 50% span location. Therefore the original geometry of the leading edge was enlarged in the direction of the airfoil thickness to fit the measured geometry and used to reproduce the geometry of the leading edge, which could not be measured. Other kinds of efforts are necessary to measure the leading edge geometry accurately.

The comparison of airfoil parameters between the original geometry and the measured geometry is conducted at several span locations in the span range from 20% to 90%. Results show that there is little difference in camber, twist angle and trailing edge angle. However the difference of the leading edge radius is remarkable between the two geometries, increasing from the inner wing to the outer wing. The leading edge radius of the measured geometry is larger by an average of 53% and up to 120% than that of the original geometry. The discrepancy is roughly from 0.01mm to 0.05mm in actual size, which is very small considering manufacturing accuracy. Also the discrepancy comes from the small radius of the leading edge especially at the outer wing. Very thin wing, which is specific to supersonic transporters and small scaled model causes such small radius at the leading edge. Figure 7 shows comparison of wing cross section shape at the 50% and 90% span locations. As for the leading edge radius, measured geometry is larger than that of the original geometry. The airfoil shape itself is quite different from the measured geometry at the 90% span location because the discrepancy of the leading edge radius is relatively bigger comparing to airfoil thickness. Moreover, symmetry of the airframe is lost because its right and left wing have different cross sections Thus this discrepancy of the model geometry mentioned above is one of the main reason for the discrepancy of pressure distributions.

The calculation for the measured geometry was conducted for both sides of the airframe because of the discrepancy of the left and right wing shape. All the other calculations for the original geometry were conducted for one side of the airframe because of the symmetry. As for the pres-



(a) $y/b = 50\%$



(b) $y/b = 90\%$

Fig. 7 Comparison of the airfoil geometry

sure measurement, pressure distributions on the upper surface were measured on the left wing and those of the lower surface were measured on the right wing. The results of the measured geometry are shown as the legend of "SA-3dm" in Fig. 8 and 9. Here, "SA" in the legend means that SA model was used as a turbulence model. As for the calculation results, there is another difference between the original geometry and the measured geometry. The actual wind tunnel model has the trailing edge thickness. Therefore, calculations for the measured geometry considered this thick-

ness, which are ignored in all the other calculations for the original geometry. This difference is appeared in C_D . C_D of the measured geometry is about 6 counts larger than that of the original geometry. This difference of 6 counts is caused by the effect of the discrepancy of the wing geometry as well as the effect of the trailing edge thickness. As for other aerodynamic characteristics, C_L and C_M , there is no remarkable difference between both geometries. While, effects on the pressure distributions are remarkable, which brings the pressure distributions of the CFD results close to those of the experimental data at both 50% and 90% span locations.

Here, we would insist that this wind tunnel model is not an inferior product but the product which can fully satisfy the accuracy requirement for honor of manufacturer. What we learned from this study is that it is necessary to reconsider the accuracy requirement of the wind tunnel models in several cases such as leading edge, thin wing, etc..

3.5 Aeroelastticity

Aeroelastic analysis was conducted to check an elastic deformation effect of the wind tunnel model. Its fuselage, tail wings and inner wing were fixed and the elastic model was made for the outer wing (from the 40% span location to the tip). Further details about this analysis method can be found in another paper[8]. The results of the deformed shape, which were obtained from the aeroelastic analysis, are shown as the legend of "BL-elas" in Fig. 8 and 9. Here, "BL" in the legend means that BL model was used as a turbulence model. The aeroelastic effect decreases both C_L and $C_{L\alpha}$ and increases C_M and $C_{M\alpha}$, bringing the CFD results close to the experimental data. In this analysis, only the deformation of the outer wing is considered. Therefore, it brings the CFD results more close to the experimental data to consider the deformation of the entire wing and the fuselage. On the other hand, the aeroelastic deformation doesn't affect pressure distributions so much.

3.6 Transition specification

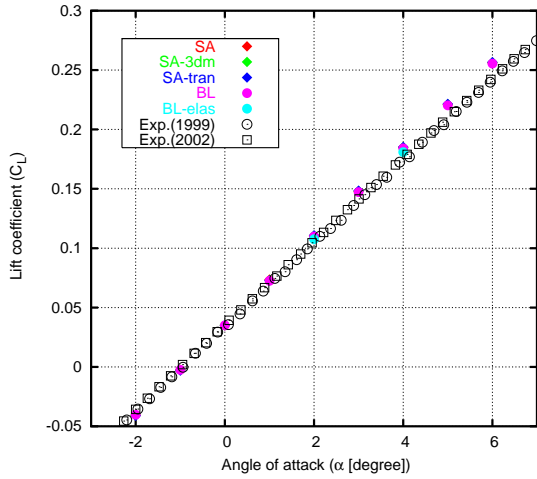
A simple transition model was used to investigate the effect of the transition, which switches off the production term in Spalart-Allmaras turbulence model at the laminar region. In the experiment, roughness was put on at the 3% cord position for all wings and at the 5% overall length for fuselage in order to force the transition from the laminar flow into turbulence flow. These positions of the roughness are set as the transition positions in the calculations. The results are shown as the legend of "SA-tran" in Fig. 8 and 9. Comparing the results with the transition to those without the transition, there is no remarkable difference for the aerodynamic characteristics. On the contrary, the transition effect is remarkable for the pressure distributions at the 50% span location, which brings the CFD results close to the experimental data.

Now, we summarize as follows (cf. table 5).

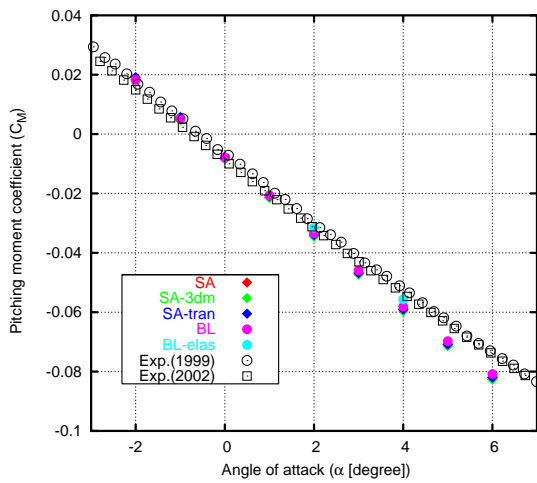
1. The discrepancy of $C_{L\alpha}$ and $C_{M\alpha}$ can be decreased by considering the aeroelastic deformation of the wind tunnel mode.
2. The discrepancy of the pressure distributions at the 50% span location can be decreased by considering the measured geometry of the wind tunnel model and the transition specification.
3. The discrepancy of the pressure distributions at the 90% span location can be decreased by considering the measured geometry of the wind tunnel model.

Table 5 Summary of studies

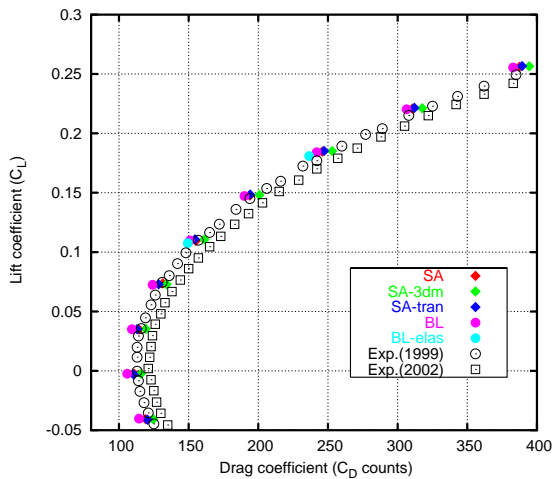
section	subjects	influence on		Fig.
		C_L, C_D, C_M	C_p	
3.2	M_∞ and α			5,6
3.3	repeatability	C_D		8
3.4	geometry	C_D	○	8, 9
3.5	aeroelasticity	$C_{L\alpha}, C_{M\alpha}$		8
3.6	transition		○	9



(a) Lift coefficient (C_L)

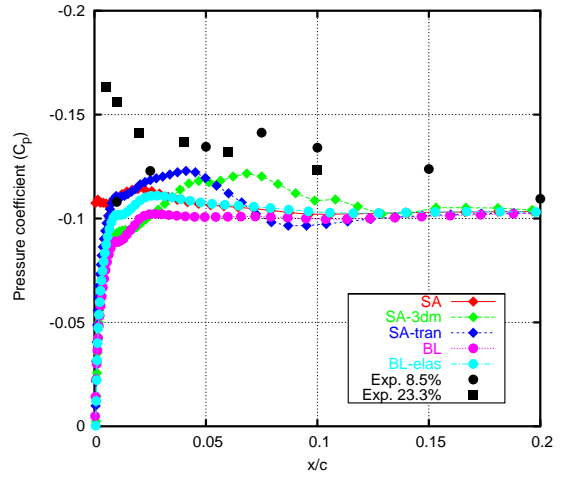


(b) Pitching moment coefficient (C_M)

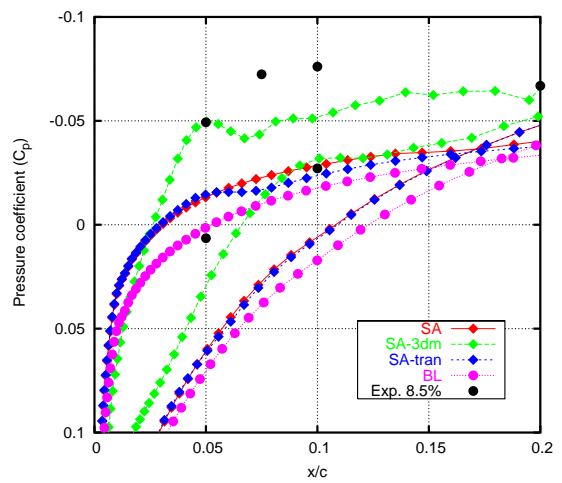


(c) Drag polars

Fig. 8 Comparison of the aerodynamic characteristics



(a) $\alpha = 2$ and $y/b = 50\%$



(b) $\alpha = 0$ and $y/b = 90\%$

Fig. 9 Comparison of the pressure distributions at the leading edge

In this study, each subject is studied independently in order to verify each effect. The discrepancy between the CFD results and the experimental data can be greatly reduced if all the following subjects are considered concurrently, the measured geometry, the elastic deformation and the transition specification.

The discrepancy of the pressure distributions at the leading edge is due to the very small difference like 0.05mm of the geometry. This size is the same as the paint thickness of the wind tunnel model, which is about 0.03mm. In other words, the pressure distributions at the leading edge is strongly affected by the geometry difference of the same order as the paint thickness. This fact

suggests that particular attention should be given to the accuracy requirement and manufacturing accuracy to the wind tunnel model as well as the paint thickness when pressure or temperature sensitive paint is used especially for the leading edge shape.

4 Conclusions

Detailed comparison of the CFD results and the experimental data was conducted as for the aerodynamic characteristics and the pressure distributions of the supersonic flow around NEXST-1. The CFD results shows good agreement with each other. The CFD results and the experimental data show good agreement except for the discrepancies of $C_{L\alpha}$, $C_{M\alpha}$, and pressure distributions at the leading edge and the outer wing. Our conclusions are as follows.

1. The discrepancy of $C_{L\alpha}$ and $C_{M\alpha}$ comes from the aeroelastic deformation of the wind tunnel mode.
2. The discrepancy of the pressure distributions at the 50% span location comes from the difference of the model geometry and the transition specification.
3. The discrepancy of the pressure distributions at the 90% span location comes from the difference of the model geometry.

The drag estimation error required in the aerodynamic design is less than 1 count. This requirement is still very severe for the current CFD technology. However, this study shows the estimation error of CFD is not greatly inferior to the experimental data in this case. The experimental data with high quality are necessary for further validation of CFD. For this purpose, it is important to establish further collaboration between CFD and wind tunnel testing. CFD should be used to clarify several problems of wind tunnel tests and help the establishment of the correction method to eliminate the interaction of wind tunnel walls and support devices. Collaboration can lead both CFD and wind tunnel tests to have high reliability.

References

- [1] K. Sakata. Supersonic Research Program in NAL, Japan. In *1st CFD Workshop for Supersonic Transport Design*, 1998.
- [2] *International Workshop on Numerical Simulation Technology for Design of Next Generation Supersonic Civil Transport 2001 – 3rd SST-CFD-Workshop –*, December 2001. Tokyo, JAPAN.
- [3] R. Takaki, K. Yamamoto, and K. Yoshida. Comparison of CFD Results for the Flow Around NEXST-1 – Detailed Study on CFD Results at 3rd SST-WS –. In *Proceedings of Aerospace Numerical Simulation Symposium 2002*, pages 81–88. NAL SP-57, 2003. in Japanese.
- [4] R. Takaki, K. Yamamoto, T. Yamane, S. Enomoto, and J. Mukai. The Development of the UPACS CFD Environment. In A. Veidenbaum, K. Joe, H. Amano, and H. Aiso, editors, *High Performance Computing, 5th International Symposium, ISHPC 2003, Tokyo-Odaiba, Japan, October 2003. Proceedings*, volume 2858 of *Lecture Notes in Computer Science*, pages 307–319. Springer, 2003.
- [5] H. Ishikawa, R. Takaki, M. Noguchi, and K. Yoshida. Comparison of the wind tunnel test and CFD of the Non-powered scaled supersonic experiment airplane. In *Proceedings of The 40th Aircraft Symposium IB7*, 2002. in Japanese.
- [6] N. Suzuki, M. Sato, H. Kanda, and N. Watanabe. Supersonic wind tunnel testing plane of the next-1 – subject on mutual validation work between efd and cfd. In *Proceedings of Aerospace Numerical Simulation Symposium 2002*, pages 94–99. NAL SP-57, 2003. in Japanese.
- [7] S. Jeong, R. Takaki, and K. Yamamoto. Application of inverse design method to estimation of wind tunnel models. In *International Symposium on Inverse Problems in Engineering Mechanics 2003*, 2003. Nagano, JAPAN.
- [8] H. Kawakami, T. Kurotaki, R. Takaki, H. Ishikawa, and F. Kuroda. Aeroelastic Analysis of the Non-powered Supersonic Experimental Airplane at Flight Condition. In *Proceedings of The 39th Aircraft Symposium*, 2001. in Japanese.